Turk J Elec Eng & Comp Sci, Vol.17, No.3, 2009, © TÜBİTAK
doi:10.3906/elk-0908-179

Experimantal characterization and equivalent circuit extraction of nanowires for signal integrity applications

Gicelio ANTONINI[1], Marc Di CLERICO[1], Antonio ORLANDI[1]
Vittorio RICCHIUTI[2], Maurizio PASSACANTANDO[3], Sandro SANTUCCI[3]
[1] *UAq EMC Laboratory, Dept. of Electrical Engineering, Univ. of L'Aquila, L'Aquila-ITALY*
e-mail: antonini@ing.univaq.it, marcodiclerico@virgilio.it , orlandi@ing.univaq.it
[2] *TechnoLabs S.p.A. ss. 17,loc. Boschetto, L'Aquila-ITALY*
e-mail: vittorio.ricchiuti@technolabs.it
[3] *Department of Physics, University of L'Aquila, L'Aquila-ITALY*
e-mail: sandro.santucci@aquila.infn.it

Abstract

This paper illustrates the design steps of a printed circuit board used as test vehicles for the measurement of the electrical properties of carbon nanotube's deposit. The board has been built and used for the measurements. The measured data are post-processed in order to extract the required properties of the only nanotubes. An equivalent circuit is extracted for further use in EDA simulators and the IEEE P1597 Standard is used to compare the results.

1. Introduction

Carbon nanotubes (CNTs) are allotropes of carbon. A single-walled carbon nanotube (SWNT) is a one-atom thick sheet of graphite (called graphene) rolled up into a seamless cylinder with diameter on the order of a nanometer. Nanotubes are members of the fullerene structural family, which also includes buckyballs. Whereas buckyballs are spherical in shape, a nanotube is cylindrical, with at least one end typically capped with a hemisphere of the buckyball structure. Their name is derived from their size, since the diameter of a nanotube is in the order of a few nanometers (approximately 1/50,000th of the width of a human hair), while they can be up to several millimeters in length. Nanotubes are categorized as single-walled nanotubes (SWNTs) and multi-walled nanotubes (MWNTs) [1].

The nature of the bonding of a nanotube is described by applied quantum chemistry, specifically, orbital hybridization. The chemical bonding of nanotubes are composed entirely of sp^2 bonds, similar to those of graphite. This bonding structure, which is stronger than the sp^3 bonds found in diamond, provides the molecules with their unique strength. Nanotubes naturally align themselves into "ropes" held together by Van der Waals forces. Under high pressure, nanotubes can merge together, trading some sp^2 bonds for sp^3

bonds, giving great possibility for producing strong, unlimited-length wires through high-pressure nanotube linking.

This results in a nanostructure where the length-to-diameter ratio exceeds 10^6. Such cylindrical carbon molecules have novel properties that make them potentially useful in many applications in nanotechnology, electronics, optics and other fields of materials science. They exhibit extraordinary strength and unique electrical properties, and are efficient conductors of heat. Inorganic nanotubes have also been synthesized.

Since their discovery in the early 1990s [2] there has been intense activity exploring the electrical properties of these systems and their potential and innovative electronic applications as interconnection elements or for the realization of radiofrequency filters.

Experiments and theory have shown that these tubes can be either metals or semiconductors, and their electrical properties can rival, or even exceed, the best metals and semiconductors known. However, experiments to test these remarkable theoretical predictions have been extremely difficult to carry out, largely because the electronic properties are expected to depend strongly on the diameter and chirality of the nanotube and because of their nanometric dimensions.

Apart from the problems associated with making electronic or optical measurements on structures just a nanometre across, it is also important to gain information on the symmetry of the nanotube. Despite these difficulties, pioneering experimental work has confirmed the main theoretical predictions about the electronic structure of nanotubes.

So, it is necessary to realize a structure for the measurement of the electrical properties of a carbon nanotube film.

This work is focused on the design of a test vehicle to measure the macroscopic electric signal transmission properties of a deposit of nanotubes in light of possible applications as interconnection or filtering structures. The novelty contribution is in the design of the test board that allows an high repeatability of the measurements and the possibility to de-embed, with an high degree of accuracy, the contributions of the fixtures to that of the nanostructures under test.

In the next Section it is briefly described the physical characteristic of the deposit used in this study; the nanotubes are supported by a Silicon (Si) and copper (Cu) layers in form of a brick-like structure. They are grown at two different temperatures (500 °C and 700 °C) producing two different kind of nanotubes. Section III is devoted to illustrate the design of a suitable printed circuit board (PCB) on which the brick is connected by means of bond wires. Surface Mounted Adapter (SMA) connectors are used to connect the board to the measurement equipment. The target of the board is to make repeatable the measurement of Scattering parameters (S-parameters). It is inherent in this technique to measure the S-parameter between the two connectors at which the instrument is connected. Because of this it is needed to de-embed the properties of the nanotubes from the overall measurements. This is done in Section IV. The de-embedded S-parameters results for the considered nonstructures are, in Section V, processed in order to extract an equivalent circuit that represent the behaviour of the nanotubes between the two ports of measurements in a given frequency range. Section VI draws some conclusions.

2. The nanowire sample

The samples that are considered in this research work consist of a carbon nanotube film deposited on a growth substrate. This substrate is a small rectangular brick whose dimensions are 5 mm x 7 mm and consists of four

overlapping layers: the bottom layer is a metallic copper reference plane, then there is a thick layer of silicon placed between two layers of silicon nitrite (Si_3N_4). On the top surface there are finally two platinum contacts with the carbon nanotube film all around.

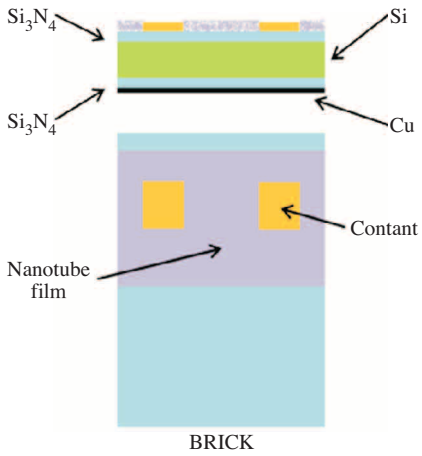

Figure 1. Cross section of the used carbon nanotube growth substrates.

The different growth direction of carbon nanotubes depends on the temperature of the substrate during the deposition process by the Chemical Vapour Deposition CVD technique [3].

In particular, if the substrate temperature is maintained equal to 500 °C, carbon nanotubes tend to grow horizontally and parallel to the substrate surface; if, instead, the temperature is set at 700 °C, carbon nanotubes tend to grow vertically.

Figure 2a and 2b are SEM images showing the carbon nanotubes deposit grown at the temperature of 700 °C. Figure 2a shows a detail of the central part of the deposit where it is possible to observe a wide range of diameters and a not perfect vertical alignment. Figure 2b presents a scanning electron microscope (SEM) image of the boundaries between the contact (left side) and the nanotube film.

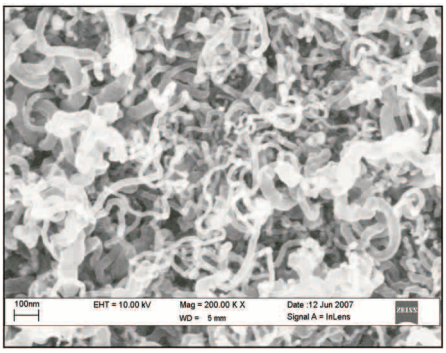

Figure 2a. SEM image of the CNTs deposit grown at 700 °C.

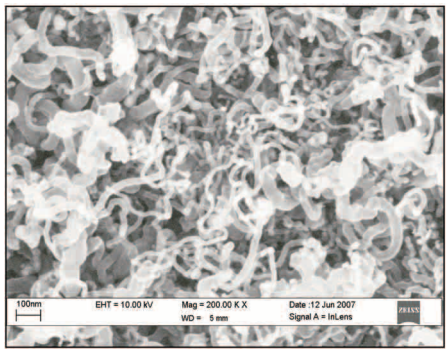

Figure 2b. SEM image of the contact interface.

3. The test board

The test vehicle is a 2 layers board whose dimensions are 200 mm x 200 mm x 0.508 mm and stack-up is in Figure 3. The dielectric material is ROGERS RO4350 (e_r = 3.48, tg d = 0.0040 @ 10 MHz). On the TOP layer are placed the bricks under test; the BOTTOM layer is a full metallized $^1/_2$ once copper plane used as reference plane.

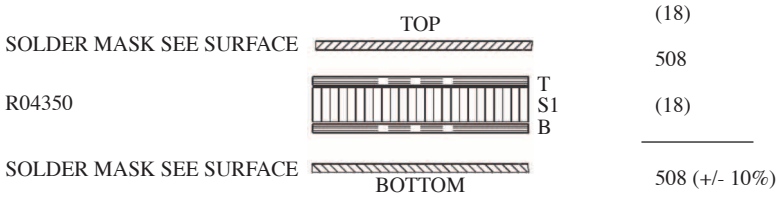

Figure 3. Test board stack-up.

The BOTTOM reference plane of the board is connected by nine through hole vias to a test pad on the TOP of the board; aside of the test pad there are also 2 pads used to solder the wire bond between the brick and the board as shown in Figures 4 and 5 shows a top view of a test pad.

The metalized bottom plane of each sample brick (on which are grown the carbon nanotube under investigation) is glued, by means of a conductive silver based glue, on the grounding pad, so that the substrate of the nanotubes is electrically connected to the reference plane of the test board. Each test pad is replicated nine time on the TOP of the board to allow multiple measurements (indicated as "Test Section" in Figure 6).

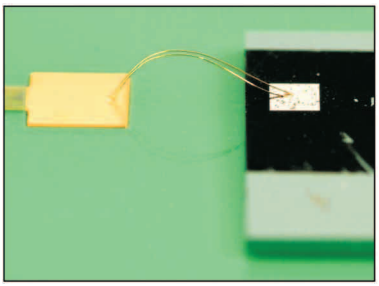

Figure 4. Soldering pad and bonding wire.

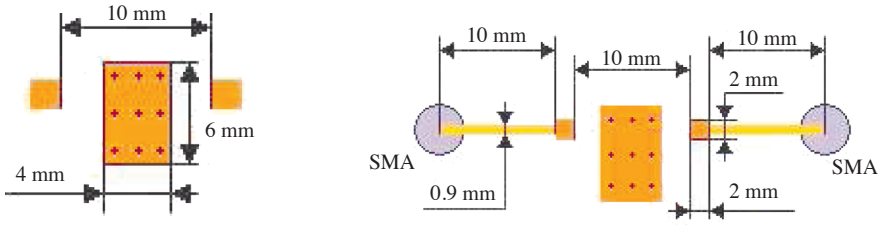

Figure 5. The test pad on the TOP: (a) with the soldering pads and (b) with the interconnections to the SMA connectors.

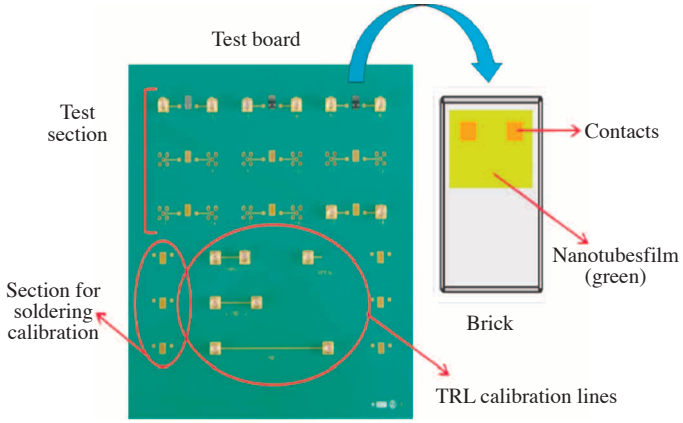

Figure 6. Test board layout.

The lower part of the test board is assigned to the calibration kits. One calibration kit is used to calibrate the thermal parameters for the soldering of the wire bonds. In this test vehicle each brick is connected to the board by two parallel gold wires with a diameter of 15 μm. The other kit is used to calibrate the Vector Network Analyze (VNA) for the measurements of the S-parameters of the device under test (DUT) de-embedding the effects of external lines and connectors. This kit is a set of four TRL (Thru-Reflect-Line) calibration lines whose parameters are specifically designed for this application.

The TRL method is a type of calibration used to perform network measurement in non-coaxial media and refers to three basic steps in the calibration process: the first step is the direct (or through a very short trace) connection of the two VNA's ports this is the THRU line (or device) designed with the same characteristic impedance of the lines that connect the DUT in the Test Section; the second step is the connection of each VNA's ports to identical high reflection coefficient devices, the OPEN line; the third step is the insertion between the two VNA's ports of a section of transmission line, the LINE device, whose length should be different from the THRU device. The designing of the TRL calibration kit requires the preliminary computation of the effective relative dielectric permittivity ε_e. According to [4]

$$\varepsilon_e = \frac{\varepsilon_r + 1}{2} + \frac{\varepsilon_r - 1}{2} \frac{1}{\sqrt{1 + 12\frac{H}{W}}} \quad \text{for } \frac{W}{H} \leq 1 \tag{1a}$$

$$\varepsilon_e = \frac{\varepsilon_r + 1}{2} + \frac{\varepsilon_r - 1}{2} \left[\frac{1}{\sqrt{1 + 12\frac{H}{W}}} + 0.04 \left(1 - \frac{W}{H}\right)^2 \right] \quad \text{for } \frac{W}{H} > 1 \tag{1b}$$

in which W is the width of the traces and H is the thickness of the dielectric (both in meters). The optimal LINE's length is a quarter wavelength or 90 degrees relative phase shift with respect the THRU line, computed at the central frequency of the chosen frequency range:

$$\text{Length}_{LINE} - \text{Length}_{THRU} = \frac{c/\sqrt{\varepsilon_e}}{2\,(f_1 + f_2)} \tag{2}$$

where c is the speed of light in the free space, and f_1 e f_2 are the start and stop frequencies of the frequency span respectively.

Since the useable bandwidth of a single THRU/LINE pair is 8:1 (frequency span / start frequency), the phase difference should remain between 20° and 160°:

$$\text{Phase Difference} = \frac{360 \cdot f \cdot (\text{Length}_{LINE} - \text{Length}_{THRU})}{c/\sqrt{\varepsilon_e}} \tag{3}$$

$f_b = \sqrt{f_1 \cdot f_2}$ If this is not achievable, that is to say the above ratio is greater than 8:1 but less than 64:1 , only two THRU/LINE pairs will be sufficient for the kit. The optimal break frequency f_b separating the two sub-bands on which the lengths of the two THRU/LINE pairs are calculated is:

$$f_b = \sqrt{f1 \cdot f_2} \tag{4}$$

In the present case the frequency range is 0.2 GHz $< f <$ 10 GHz. The lower limit is dictated by the need to constrain the length of the calibration lines into values compatible with the board's dimensions. The upper limit is dictated by the properties of the SMA connectors used: above 10 GHz their insertion loss is too high to allow a correct measurement of the S-parameters. By using the design values of $W = 0.9$ mm, $H = 0.508$ mm, $\varepsilon_r = 3.48$ a ratio $W/H > 1$ is obtained; (1b) is used to compute $\varepsilon_e = 2.68$. For the given frequency range the ratio frequency span/start frequency is equal to 49. The break frequency to separate the two sub-bands on which the THRU/LINE pairs are designed is $f_b = 1.41$ GHz.

The length of the OPEN line should be the same distance between the center conductor of the SMA connector and the soldering pad. This length has been set equal to 10 mm as an acceptable compromise between geometric constraints and loses containment. Frome the above indications the length of the calibration kit lines are:

$$\text{Length}_{OPEN} = 10\ mm \tag{5a}$$

$$\text{Length}_{THRU} = 2 \cdot \text{Length}_{OPEN} = 20\ mm \tag{5b}$$

$$\text{Length}_{LINE\,1} = 57\ mm + \text{Length}_{THRU} = 77\ mm \tag{5c}$$

$$\text{Length}_{LINE\,2} = 8\ mm + \text{Length}_{THRU} = 28\ mm \tag{5d}$$

Of the nine test pads of the test section one has been left without brick, on another it has been glued a brick without carbon nanotubes and of the remains some has been used for testing nanotubes deposits grown at the temperature of 500 °C and other nanotubes deposits grown at the temperature of 700 °C. In this way, as it will be shown in the next Section, it will be possible to observe the differences between different deposits and de-embedding the behavior of the text fixtures.

4. Measurement and results

The measurement have been performed by using the VNA Anritsu 37247C VNA in a frequency range from 0 to 10 GHz by using 1601 frequency points. After the TRL calibration process the measurements of magnitude and phase of the four scattering parameters S_{11}, S_{12}, S_{21} and S_{22} have been performed on specific test pads of the board.

The first S parameters measurement (M1) is carried out on a test pad without the presence of any brick. This is done to obtain a baseline for the other measurements. The frequency spectrum of the magnitude of the forward transmission scattering parameter S_{21} is in Figure 7.

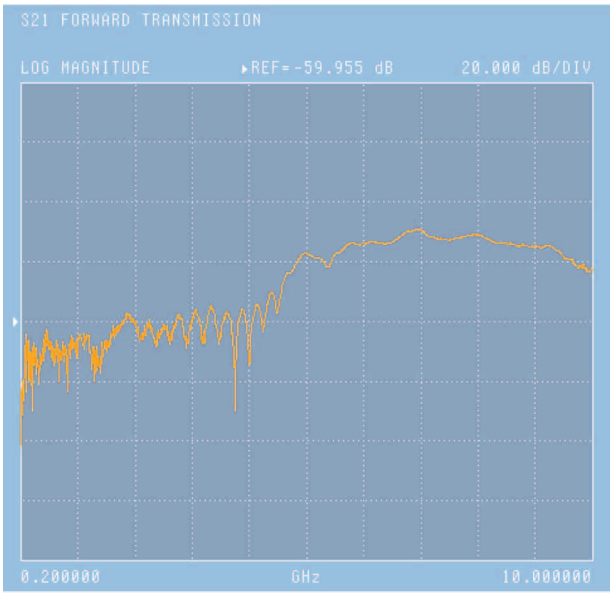

Figure 7. Measurement 1 (M1): frequency spectrum of $|S_{21}|$ (Y axis: REF. value = -60 dB, 20 dB/div; X axis: 1 GHz/div).

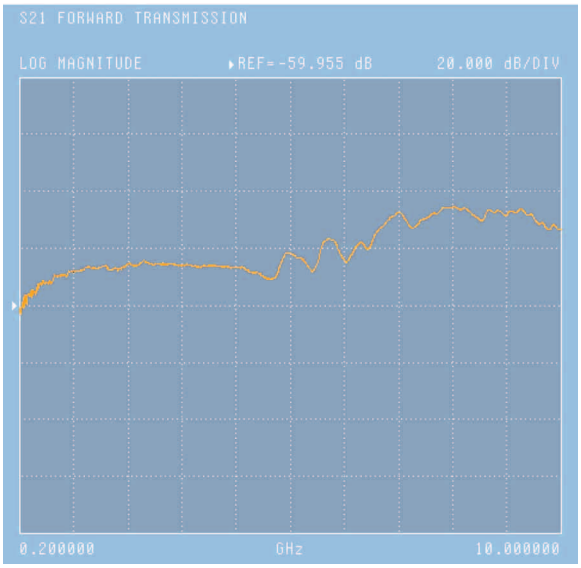

Figure 8. Measurement 2 (M2): frequency spectrum of $|S_{21}|$ (Y axis: REF. value = -60 dB, 20 dB/div; X axis: 1 GHz/div).

The second measurement (M2) has been carried out on a test pad in presence of a brick but without the CNTs deposit. The results of the measurement is in Figure 8.

Finally in the third (M3, Figure 9) and fourth (M4, Figure 10)) measurement it has been measured the forward transmission parameters for a test pad in presence of samples with CNTs deposits grown at 500 °C and 700 °C respectively.

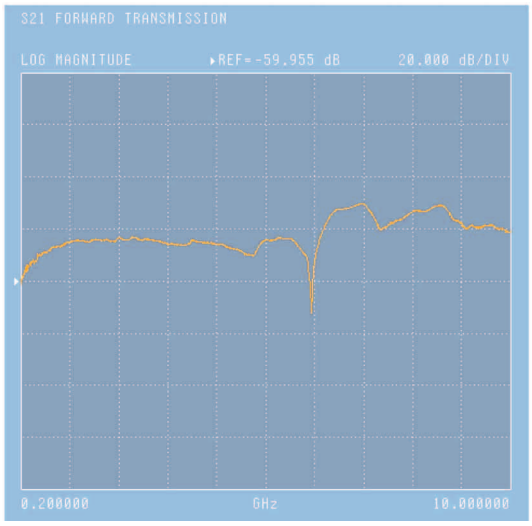

Figure 9. Measurement 3 (M3) with CNTs deposits grown at 500 °C: frequency spectrum of $|S_{21}|$ (Y axis: REF. value = -60 dB, 20 dB/div; X axis: 1 GHz/div).

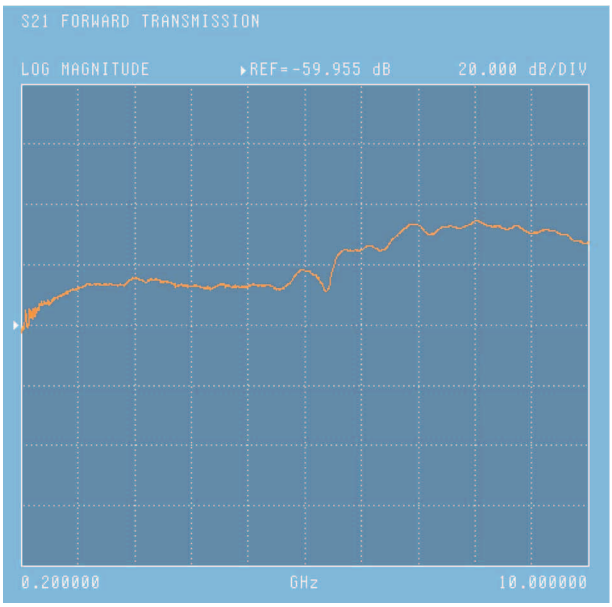

Figure 10. Measurement 4 (M4) CNTs deposits grown at 700 °C: frequency spectrum of $|S_{21}|$ (Y axis: REF. value = -60 dB, 20 dB/div; X axis: 1 GHz/div).

The comparison of the above measurement gives an idea of the behaviour of the brick with the CNT deposit in the considered frequency range. It should be noted that all the measurement are taken between the two SMA connectors and hence they include not only the CNT deposit behaviour but also the impact of the two connectors, of the two interconnections and of the two wire bonds. Because of this it turns necessary to implement a de-embedding procedure [5] in order to de-embed S_{21} of the only CNT deposit.

From M1, the $\mathbf{S}_{PAD}$ matrix (from now on bold characters indicate matrix) is converted in the admittance one $\mathbf{Y}_{PAD}$.

M2 evaluates the matrix $\mathbf{S}_{PAD//BRICK}$ (without the presence of the CNTs deposit) that is also converted into $\mathbf{Y}_{PAD//BRICK}$. From an electrical point of view, as illustrated in Figure 11, the pad and the brick are in parallel. By using the properties of the 2-port networks one has

$$Y_{BRICK} = Y_{PAD//BRICK} - Y_{PAD} \tag{6}$$

By using the reverse conversion formulas applied to the $\mathbf{Y}_{BRICK}$ matrix one compute the $\mathbf{S}_{BRICK}$ matrix of the brick without CNTs deposit.

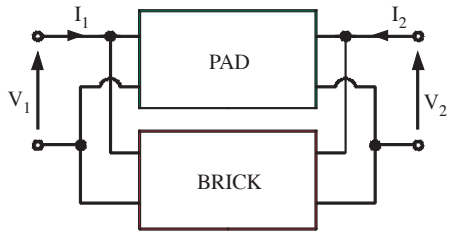

Figigure 11. 2-ports network configuration for M2.

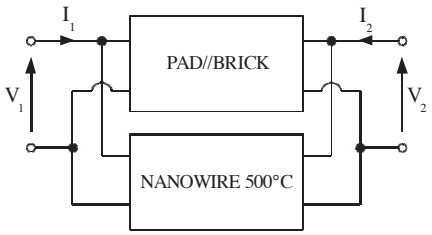

Figure 12. 2-ports network configuration for M3

M3 concerns the measurement of the S parameters at a test pad with a brick with a film of carbon nanotubes grown at 500 °C. The only difference compared to M2 measurement is the presence of the deposit. The CNTs deposit (indicated as nanowire 500°C in Figure 12) is equivalent to a two-port network in parallel with another two-port network represented by the $\mathbf{S}_{PAD//BRICK}$ matrix.

The $\mathbf{S}_{(PAD//BRICK)//NANOWIRE500°C}$ is known from the third measurement M3. By applying the S-to-Y conversion formulas one computes $\mathbf{Y}_{(PAD//BRICK)//NANOWIRE500°C}$ and also

$$Y_{NANOWIRE500°C} = Y_{(PAD//BRICK)//NANOWIRE500°C} - \mathbf{Y}_{PAD//BRICK} \tag{7}$$

By applying the reverse conversion formulas to (7) the requested scattering matrix $\mathbf{S}_{NANOWIRE500°C}$ for the CNTs grown at 500 °C is computed. The same process can be applied for the CNTs grown at 700 °C obtaining $\mathbf{Y}_{NANOWIRE700°C}$ by (7) and $\mathbf{S}_{NANOWIRE700°C}$ by the Y-to-S formulas.

Figs. 13 show the results of this de-embedding procedure for the magnitude of |S21| associated at CNTs grown at the two above mentioned temperatures.

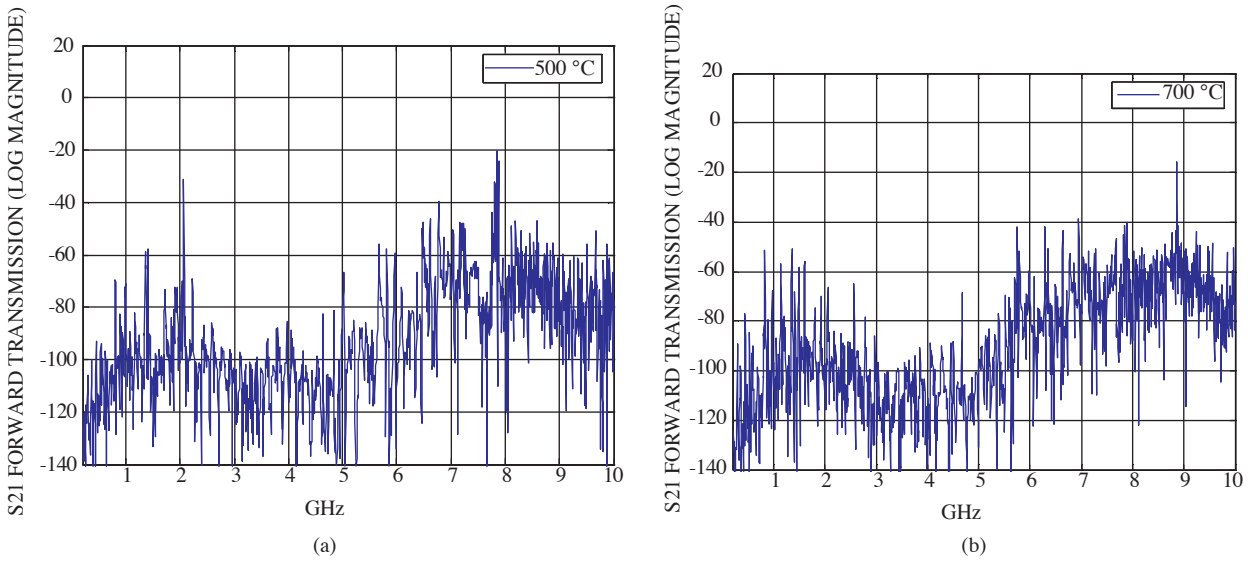

Figure 13. Frequency spectrum of $|S_{21}|$ after de-emebedding for the CNTs deposit: (a) grown at 500 °C and (b) grown at 700 °C.

The small values of $|S_{21}|$ are due to the perpendicular laying of the CNT with respect the flowing direction of the currents.

5. Equivalent circuit extraction

Nowadays in order to perform the electrical simulations of complex systems it is preferred to have them in circuit or rational (poles and residues) format. Starting from the de-embedded S-parameters of the CNTs deposits it has been extracted the circuit (in HSPICE syntax) and the rational model by using the Broad Band Generator (BBG) mode of ADS 2008 [6]. BBG uses the rational approximation

$$S_{ij}(s) = \frac{g_0 + g_1 s + g_2 s^2 + \cdots + g_\alpha s^\alpha}{1 + d_1 s + d_2 s^2 + \cdots + d_\beta s^\beta} \tag{8}$$

to fit the frequency response in terms of scattering parameters. In (8) s is the Laplace variable $s = \mathrm{j}\omega$, ω is the angular frequency, g_k are the α order real polynomial coefficients of the numerator, while d_k are the β order polynomial coefficients of the denominator. The BBG HSPICE extracted circuit is a proper collection of first or second order sub-circuits with controlled sources.

Figure 14 shows the comparison of the original frequency spectrum of $|S_{21}|$ (after de-embedding) of the CNT deposit grown at 500 °C (curve (a)) and the spectrum of $|S_{21}|$ computed by using the equivalent circuit extracted by BBG (curve (b)) with 315 poles. In order to allow a better comparison the (b) curve has been slightly shifted downward.

To quantify this comparison it has been made reference to the recent IEEE Standard for validation of computer models and simulations [7]. This Standard gives rules for a correct, robust and repeatable comparison of two different datasets, indicating the Feature Selective Validation (FSV) algorithm [8] as the suitable technique

to perform the comparison. Goal of FSV is to mimic the behaviour and judgement of a group of experts when they perform a visual comparison among different data. The three main figure of merits of FSV are the Amplitude Difference Measure (ADM) that is the measure of the differences between the general trends of the datasets, the Feature Difference Measure (FDM) that is a quantification of the differences between the details (peaks, nulls, features) of the datasets and the Global Difference Measure (GDM) a weighted combination of ADM and FDM. To apply FSV it has been used the FSV Tool (see Figure 15), a software tool developed for this purpose and freely downloadable from [9,10].

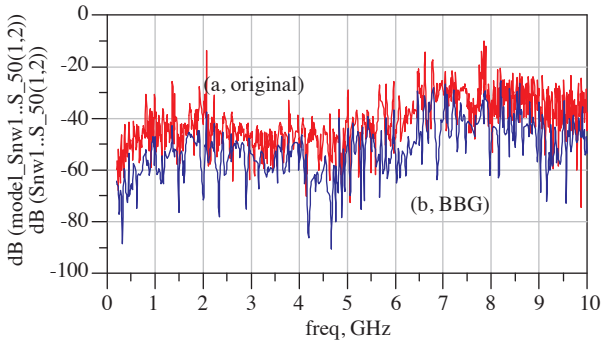

Figure 14. Frequency spectrum of |S21| for 500° C CNTs deposit: (a) measured data after de-embedding and (b) data obtained by the BBG extracted equivalent circuit.

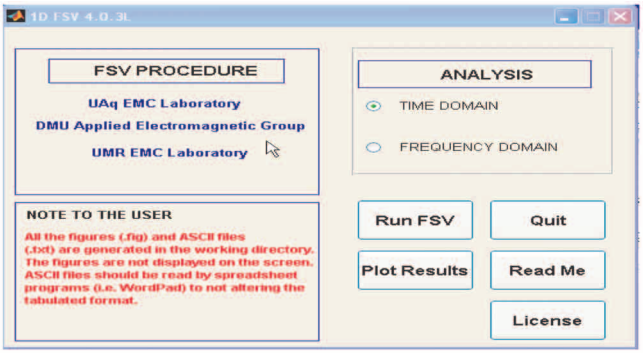

Figure 15. Frontend of the FSV Tool.

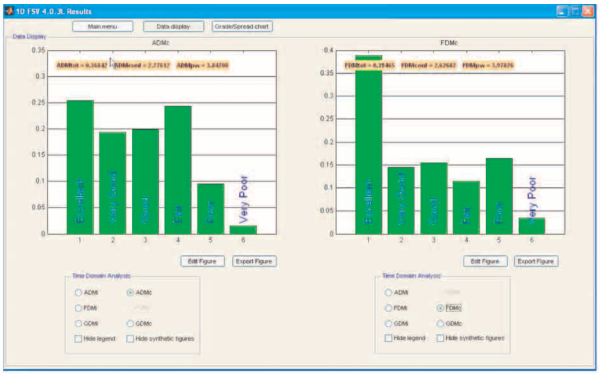

Figure 16. ADM_c and FDM_c for data comparison in fig. 14.

Figures 16 and 17 show the output of the FSV technique. Figure 16 offers the confidence levels of ADM (left) and FDM (right) indicating the number of points' pair in Figure 14 whose comparison fall into the 6 FSV classes, ranging from EXCELLENT to VERY POOR comparison. For both distributions it is visible as the centroid is well shifted toward the left side, that is to say toward the high quality of the comparison of either the trend and the features of the S parameters (original and extracted) of Figures 14 and 17 summarizes these results by using two figure of merits: the GRADE of the comparison, its overall quality (smaller it is this value better is the comparison) and the SPREAD of the value in the classes (smaller it is this value, more reliable is the result of the comparison).

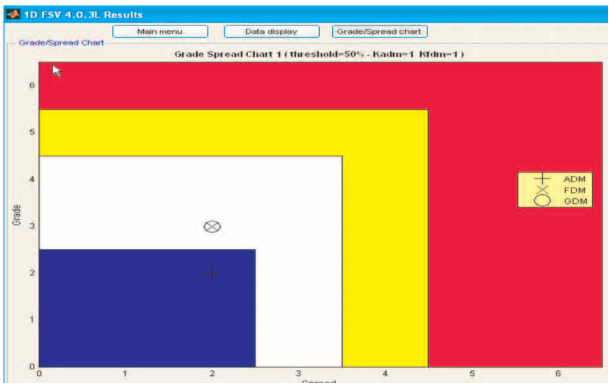

Figure 17. GRADE and SPREAD for the comparison in Figure 14.

6. Conclusions

In this paper it has been illustrated the design of a test board to perform an electrical characterization, in terms of scattering parameters, of small deposits of CNTs grown at different temperatures. The characterization it has been carried out up to 10 GHz. A de-embedding procedure it has been adopted to isolate the proper behaviour of the CNT and the recent IEEE Standard it has been adopted to quantify the results.

Acknowledgment

Authors wish to thank Dr. Silvio Perri with CREO (Research Center Electro-Optical, L'Aquila) for helping in the soldering of the wire bonds and Ing. R.M.Rizzi of *UAq EMC Laboratory* for the technical discussions.

References

[1] Website on Nanotechnology: http://nanosatyadhar.webs.io/. or http://www.chemie.de/lexikon/e/Carbon_nanotube/.

[2] D. S. Bethune, C. H. Kiang, M. S. Devries, G. Gorman, R. Savoy, J. Vazquez, and R. Beyers, "Cobalt-catalyzed growth of carbon nanotubes with single-a tomic-layerwalls," *Nature*, vol. 363, pp. 605-607, 1993.

[3] M.F.Bevilacqua, *Chemical Vapour Deposition of carbon nanotubes on iron- patterned substrate: towards a control of the positioning and structure,* Ph.D Thesis, University of Naples " Federico II", Naples, Italy, 2006.

[4] K.C.Gupta and all., Microstrip Lines and Sloitlines, II Edition, Artech Hous, London, 1996."

[5] G.Antonini, A.Orlandi, V.Ricchiuti, "De-embedding methods for characterizing PCB interconnections", in *Proc. of 9 th IEEE Workshop on Signal Propagation on Interconnects*, Garmish-Partenkirchen, Germany, May, 2005.

[6] Agilent EESof, Advanced Design System, http://eesof.tm.agilent.com/products/ads_main.html

[7] IEEE Standard P1597, Standard for Validation of Computational Electromagnetics Computer Modeling and Simulation, Part I and II, 2008.

[8] A.P.Duffy, A.J.M.Martin, A.Orlandi, G.Antonini, T.M. Benson, M.S. Woolfson, "Feature Selective Validation (FSV) for Validation of Computational Electromagnetics (CEM)", Part I and Part II, in *IEEE Transactions on Electromagnetic Compatibility*, vol. 48, n. 3, August 2006.

[9] FSV 1D: http://uaqemc.ing.univaq.it/uaqemc/FSV_4_0_3L/

[10] FSV 2D: http://uaqemc.ing.univaq.it/uaqemc/FSV_2D_2_0_6L/